Dynamical Structure of the 2/1 Commensurability with Jupiter and the Origin of the Resonant Asteroids

Michèle Moons

Département de mathématique, FUNDP, 8 Rempart de la Vierge, B-5000 Namur, Belgique

Alessandro Morbidelli

Observatoire de la Côte d'Azur, CNRS, B.P. 4229, 06304 Nice Cedex 4, France
E-mail: morby@obs-nice.fr

and

Fabio Migliorini

Armagh Observatory, College Hill, BT61 9DG Armagh, Northern Ireland, UK

Using a semi-analytic approach, we provide a three-dimensional picture of the secular dynamics in the 2/1 mean-motion commensurability, mapping the most chaotic regions and the two islands of *quasi-regular* motion. Five asteroids have recently been discovered in one of these islands and it has been conjectured that they were injected by the Themis-family formation event, which occurred close to the 2/1 resonance border. We show that this scenario is viable from the orbital and size distribution point of view and that it would also explain why no asteroids have been observed in the second island. Finally we discuss the possibility that the 2/1 resonance is the dominating source of CI and CM meteorites, as was suggested on spectroscopical bases. We find that the efficiency of the 2/1 resonance is far too small for it to be such a dominating source. © 1998 Academic Press

Key Words: asteroids; Kirkwood gaps.

1. INTRODUCTION

The origin of the Kirkwood gap associated with the 2/1 commensurability with Jupiter is one of the most challenging problems in modern celestial mechanics.

As in the framework of the planar–circular restricted three-body problem this resonance is stable, Henrard and Lemaître (1983) proposed a model in which the dissipation of the primordial nebula resulted in an outward migration

During the final revisions of this paper two tragedies occurred. Fabio Migliorini died on November 2, 1997, during a mountain hike and Michèle Moons died on January 8, 1998, after a long illness. They were respectively 26 and 46. The present paper is dedicated to their memory.

of the 2/1 resonance location with consequent ejection of resonant asteroids. However, this model could not explain why the resonance was not refilled with new asteroids, originated as collisional fragments of impacted fairly large parent bodies located in its proximity, and hence it has not been acknowledged as the ultimate solution of the 2/1 Kirkwood-gap puzzle.

Other investigations in the framework of the planar–elliptic problem (Giffen 1973, Froeschlé and Scholl 1976, Lemaître and Henrard 1990) resulted in finding a local source of chaos in the low-eccentricity part of the resonance, but no global-instability mechanism which could account for a gravitational origin of the gap. The discovery that secular resonances exist inside the 2/1 commensurability (Morbidelli and Moons 1993) renewed the interest in this problem. In that paper, the location and the dynamical effects of the ν_5, ν_6, and ν_{16} and the Kozai secular resonance were investigated using perturbation theory. We recall here briefly that the ν_5 and the ν_6 resonances occur when the averaged frequency of the asteroid's perihelion longitude is equal to the planetary proper frequencies g_5 and g_6, respectively; the ν_{16} resonance occurs whenever the averaged frequency of the asteroid node is equal to the planetary proper frequency s_6; the Kozai resonance is the 1/1 commensurability between the precession rates of the asteroid longitudes of perihelion and node.

Asteroid dynamics inside the 2/1 commensurability can be described by three coordinates: the eccentricity e and the inclination i and the action J_σ related to the amplitude of libration within the resonance. Due to the complexity of the problem, Morbidelli and Moons (1993) restricted the inves-

tigation of secular resonances to the plane $i = 0$ and to the plane $J_\sigma = 0$. Despite their simplifications, they succeeded in showing that the high-eccentricity region of the 2/1 commensurability ($e > 0.4$) is globally unstable (the eccentricity can eventually be forced up to ~1, leading the body to collide with the Sun) and that there are local channels where the asteroid inclination can be pumped up to large values (20°–30°). This investigation was extended by Henrard *et al.* (1995) where the restriction $J_\sigma = 0$ was removed, achieving analytically a description of secular-resonance dynamics for moderate values of libration amplitude, whilst the region with large J_σ was numerically studied using the Extended Schubart Integrator (Moons 1994). This approach led to the understanding of how asteroids starting in the chaotic low-eccentricity portion of the 2/1 commensurability can reach large eccentricities through a preliminary increase of inclination and libration amplitude, a phenomenon first pointed out by means of numerical integration by Wisdom (1987). Even so, at the light of this study, a region of regular motion, divided by the ν_{16} resonance into two separate islands (Moons 1997), still appeared to exist at moderate eccentricity, inclination, and libration amplitude.

However, numerical investigations (Franklin 1994, Ferraz-Mello, 1994) showed that such islands are not really regular: Lyapunov exponents are chiefly positive, although much smaller than in the regions in which secular resonances are located. These results have recently been improved, using frequency analysis (Laskar 1996, Šidlichovský and Nesvorný 1997), by Nesvorný and Ferraz-Mello (1997), who obtained a map of the different degrees of chaoticity on the plane $i = 0$. The regular islands of Henrard *et al.* (1995) turn out to be globally chaotic, so that they will be regarded hereafter as the *quasi-regular islands*.

Due to such a global chaoticity and the absence of regular trajectories, all orbits should diffuse and eventually escape (Morbidelli and Guzzo 1997), and the long-term integration of the dynamical evolution of a few fictitious particles can reveal the escape-process time scales. Morbidelli (1996) integrated for 1 Gyr 24 test particles in the 2/1 commensurability with initial $e < 0.355$ and $i < 1.5°$. The median-particle lifetime was of the order of 80 Myr, while in the quasi-regular island typical lifetimes were much longer (order of several 10^8 yr or possibly longer). Note that 4 of the 24 particles survived 1 Gyr without escaping to the high-e regions of the 2/1 commensurability.

Unfortunately, the numerical analysis by Nesvorný and Ferraz-Mello (1997) is too time-consuming for the current computer capability to achieve a global three-dimensional picture of the dynamics in the 2/1 resonance, namely to extend their analysis from moderate up to large inclinations. As a consequence, only two pictures concerning the dynamics on the (e, i)-plane at two different libration amplitudes have been published.

This leads us to believe that it is timely to provide the first global three-dimensional picture of the location and amplitude of the main secular and secondary resonances, since it is now clear that they constitute the skeleton of the dynamics in the 2/1 commensurability. In the next section we shall explain our analytical approach, whereas in Section 3 we shall emphasize our results. The 3-D picture of secular and secondary resonances will allow us to combine previous results.

In Section 4 we shall quantitatively investigate the hypothesis that the long-living asteroids, partially recognized in 1996 by Morbidelli and in 1997 by Nesvorný and Ferraz-Mello to be associated with one of the quasi-regular islands, could be the remnant of the Themis-family breakup event which occurred near the 2/1 resonance border (Morbidelli *et al.*, 1995).

Last, in Section 5, we shall discuss the possibility that the 2/1 commensurability is the source of CI and CM meteorites.

2. 3-D STUDY OF THE DYNAMICS

This technical section is aimed at illustrating our perturbation approach to the localization and the size of secular and secondary resonances with no restrictions on eccentricity, inclination and amplitude of libration in the 2/1 resonance. As a matter of fact, our approach is very similar to that illustrated in Section 2 of Morbidelli and Moons (1993), with the main difference that we shall not restrict here to the case $J_\sigma \rightarrow 0$. Readers interested merely in the results can go directly to Section 3.

We shall begin as usual with the Hamiltonian of the restricted three-body problem Sun–Jupiter–asteroid,

$$\mathcal{H} = L' - \frac{1 - \mu}{2a} - \mu \left(\frac{1}{|\mathbf{r} - \mathbf{r}'|} - \frac{\mathbf{r}|\mathbf{r}'}{r'^3} \right),$$

where $\mathbf{r}$ is the heliocentric position vector of the asteroid, $\mathbf{r}'$ the one of Jupiter, μ the mass of Jupiter, L' the conjugate momentum to the mean longitude of Jupiter, and a the asteroid semi-major axis. The universal gravitational constant, the semi-major axis of Jupiter, and the total mass of the Sun–Jupiter system are chosen as units (clearly the asteroid is regarded as a massless point).

We immediately extend the problem in order to account with the secular variations of Jupiter orbital elements due to the presence of Saturn:

$$e' \cos \varpi' = m_{5,5} \cos(g_5 t + \lambda_5^0) + m_{5,6} \cos(g_6 t + \lambda_6^0)$$

$$e' \sin \varpi' = m_{5,5} \sin(g_5 t + \lambda_5^0) + m_{5,6} \sin(g_6 t + \lambda_6^0)$$

$$\sin \frac{i'}{2} \cos \Omega' = n_{5,6} \cos(s_6 t + \mu_6^0)$$

$$\sin \frac{i'}{2} \sin \Omega' = n_{5,6} \sin(s_6 t + \mu_6^0).$$

(1)

Adopted values for the constants $m_{5,5}, g_5, \lambda_5^0, m_{5,6}, g_6, \lambda_6^0,$ $n_{5,6}, s_6,$ and μ_6^0 are taken from the LONGSTOP numerical integration of the outer Solar System (Nobili *et al.* 1989).

With the introduction of appropriate resonance variables for the 2/1 mean-motion resonance and of three new momenta conjugated to the three new time dependences introduced by the Jupiter–Saturn system, the seven-degree-of-freedom autonomous Hamiltonian of the problem reads as

$$\mathscr{H} = \Lambda' + g_5\Lambda_5' + g_6\Lambda_6' + s_6\Lambda_{16}' - 2L - \frac{1-\mu}{2a}$$
$$- \mu\left(\frac{1}{|\mathbf{r} - \mathbf{r}'|} - \frac{\mathbf{r}|\mathbf{r}'}{r'^3}\right), \tag{2}$$

being the phase space described by the set of conjugated action-angle variables

$$
\begin{aligned}
S &= L - G, & \sigma &= 2\lambda' - \lambda - \tilde{\omega} \\
S_z &= G - H, & \sigma_z &= 2\lambda' - \lambda - \Omega \\
N &= 2L - H, & \nu &= -2\lambda' + \lambda \\
\Lambda' &= 2L + L', & \lambda' & \\
\Lambda_5', & & \tilde{\omega}_5' &\equiv g_5 t \\
\Lambda_6', & & \tilde{\omega}_6' &\equiv g_6 t \\
\Lambda_{16}', & & \Omega' &\equiv s_6 t,
\end{aligned} \tag{3}
$$

where we choose the usual notations for the keplerian elements of the asteroid (primed variables for Jupiter): a for the semi-major axis, e for the eccentricity, i for the inclination, λ for the mean longitude, $\tilde{\omega}$ for the longitude of perihelion, and Ω for the longitude of node, and where $L = \sqrt{(1-\mu)a}$, $G = L\sqrt{1-e^2}$, and $H = G\cos i$ are the usual Delaunay's momenta.

Of the variables in (3), only λ' can be considered a fast angle. Averaging over λ' (and dropping Λ' as a constant) the Hamiltonian takes the form

$$\mathscr{H} = g_5\Lambda_5' + g_6\Lambda_6' + s_6\Lambda_{16}'$$
$$+ \mathscr{F}(\sigma, S, \sigma_z, S_z, \nu, N, \tilde{\omega}_5', \tilde{\omega}_6', \Omega'). \tag{4}$$

We now continue according to a perturbation scheme which is particularly suitable when the dynamics is characterized by a hierarchy of degrees of freedom (Morbidelli 1993). This can be schematized as follows: given a Hamiltonian problem,

$$H(p, q) = H_0(p) + H_1(p, q), \tag{5}$$

we split H_1 into $\hat{H}_1$ and $(H_1 - \hat{H}_1)$, choosing $\hat{H}_1$ such that (i) $H_0(p) + \hat{H}_1(p, q)$ is integrable and (ii) the dynamics described by $H_0(p) + \hat{H}_1(p, q)$ is the dominating character of the dynamics described by H. Then we introduce action-angle variables I, φ such that $H_0 + \hat{H}_1 \equiv F_0(I)$; note that the existence of such variables is proved by the Arnold–Liouville theorem (Arnold 1963). Letting the expression of $(H_1 - \hat{H}_1)$ in the new variables, be denoted by F_1, (5) becomes

$$F = F_0(I) + F_1(I, \varphi). \tag{6}$$

The Hamiltonian (6) has the same form as (5), so the procedure can be iterated until a good description of the dynamics is achieved. It has been proved (Morbidelli and Giorgilli 1993) that the infinite iteration of the procedure would converge on the invariant KAM tori of the system.

In our specific problem (4), the dominating integrable dynamics is the one related to the 2/1 mean-motion resonance (i.e., to the angle σ). Therefore, we separate all terms which are independent of σ_z, ν, ω_5', ω_6', and Ω'; namely we write $\mathscr{F} = \mathscr{F}_\sigma + (\mathscr{F} - \mathscr{F}_\sigma)$, where

$$\mathscr{F}_\sigma(\sigma, S, S_z, N) = \int\int\int\int \mathscr{F} d\sigma_z \, d\tilde{\omega}_5' \, d\tilde{\omega}_6' \, d\Omega' \tag{7}$$

(the integral over ν is useless because, for the D'Alembert characteristics, ν is always coupled to either $\tilde{\omega}_5'$ or $\tilde{\omega}_6'$ or Ω' in the Fourier expansion of $\mathscr{F}$). The Hamiltonian

$$\mathscr{H}_\sigma = g_5\Lambda_5' + g_6\Lambda_6' + s_6\Lambda_{16}' + \mathscr{F}_\sigma \tag{8}$$

is integrable, since it depends only on one angle. Now we introduce new action-angle variables

$$
\begin{aligned}
\psi_\sigma &= \frac{2\pi}{T_\sigma}t, & J_\sigma &= \frac{1}{2\pi}\oint S \, d\sigma \\
\psi_z &= \sigma_z - \rho_z(\psi_\sigma, J_\sigma, J_z, J_\nu), & J_z &= S_z \\
\psi_\nu &= \nu - \rho_\nu(\psi_\sigma, J_\sigma, J_z, J_\nu), & J_\nu &= N,
\end{aligned} \tag{9}
$$

such that $\mathscr{H}_\sigma$ becomes dependent only on the action variables; i.e.,

$$\mathscr{H}_\sigma \equiv \mathscr{F}_0(\Lambda_5', \Lambda_6', \Lambda_{16}', J_\sigma, J_z, J_\nu). \tag{10}$$

Since we are interested in the dynamics *inside* the 2/1 commensurability, we compute the separatrices of $\mathscr{H}_\sigma$ in the (σ, S, S_z, N)-space and introduce the variables (9) only for trajectories with librating σ, so that T_σ is the period of libration and J_σ is the normalized area bounded by the librating trajectory in the (S, σ) plane. We recall that the

functions ρ_z and ρ_ν are periodic in ψ_σ and are introduced in order to keep (9) in canonical form (see Henrard 1990).

Substituting the new variables (9) in the neglected term $\mathscr{F}_1 \equiv \mathscr{F} - \mathscr{F}_\sigma$, the full Hamiltonian (4) becomes

$$\mathscr{H} = \mathscr{F}_0(\Lambda'_5, \Lambda'_6, \Lambda'_{16}, J_\sigma, J_z, J_\nu) \\ + \mathscr{F}_1(\psi_\sigma, \psi_z, \psi_\nu, \tilde{\omega}'_5, \omega'_6, \Omega', J_\sigma, J_z, J_\nu). \quad (11)$$

The dominating integrable dynamics in (11) is now the one related to the motion of ψ_z (recall that inside the 2/1 commensurability, where σ librates around 0, ψ_z is close to the perihelion argument $\omega = \tilde{\omega} - \Omega$, so that the dominating dynamics is the so-called *Kozai* dynamics). Therefore, we isolate the part which depends only on ψ_z, namely writing $\mathscr{F}_1 = \mathscr{F}_z + (\mathscr{F}_1 - \mathscr{F}_z)$, where

$$\mathscr{F}_z(\psi_z, J_\sigma, J_z, J_\nu) = \int \int \int \int \mathscr{F}_1 \, d\psi_\sigma \, d\tilde{\omega}'_5 \, d\tilde{\omega}'_6 \, d\Omega' \quad (12)$$

(again, as in (7), the integral over ψ_ν is useless because of the D'Alembert characteristics). The Hamiltonian

$$\mathscr{H}_z = \mathscr{F}_0 + \mathscr{F}_z \quad (13)$$

is integrable because it depends on only one angle (ψ_z). However, this is a resonant Hamiltonian (the Kozai resonance is present inside the 2/1 commensurability; see Jeffreys and Standish 1972). Therefore, we compute its separatrices in the (ψ_z, J_σ, J_z, J_ν)-space and we proceed to introduce in each of its topological regions (positive or negative circulation, libration of ψ_z) action-angle variables

$$\vartheta_z = \frac{2\pi}{T_z} t, \qquad\qquad \Theta_z = \frac{1}{2\pi} \oint J_z \, d\psi_z$$

$$\vartheta_\sigma = \psi_\sigma - \rho'_\sigma(\vartheta_z, \Theta_\sigma, \Theta_z, \Theta_\nu), \qquad \Theta_\sigma = J_\sigma \quad (14)$$

$$\vartheta_\nu = \psi_\nu - \rho'_\nu(\vartheta_z, \Theta_\sigma, \Theta_z, \Theta_\nu), \qquad \Theta_\nu = J_\nu,$$

such as to make $\mathscr{H}_z$ dependent only on the action variables; i.e.,

$$\mathscr{H}_z \equiv \mathscr{H}_0(\Lambda'_5, \Lambda'_6, \Lambda'_{16}, \Theta_\sigma, \Theta_z, \Theta_\nu). \quad (15)$$

when the new variables (14) are substituted into the neglected term $\mathscr{H}_1 \equiv \mathscr{F}_1 - \mathscr{F}_z$, the Hamiltonian (11) takes the form

$$\mathscr{H} = \mathscr{H}_0(\Lambda'_5, \Lambda'_6, \Lambda'_{16}, \Theta_\sigma, \Theta_z, \Theta_\nu) \\ + \mathscr{H}_1(\vartheta_\sigma, \vartheta_z, \vartheta_\nu, \tilde{\omega}'_5, \tilde{\omega}'_6, \Omega', \Theta_\sigma, \Theta_z, \Theta_\nu). \quad (16)$$

Note that since $\mathscr{H}_z$ has three distinct topological regions,

we have to introduce three different transformations of type (14) to end up with three different Hamiltonians of type (16), each of them defined in one of the topological regions.

We could have iterated the above illustrated procedure forward, looking for a new dominating degree of freedom. However, for sake of simplicity, we isolate the harmonics with argument $\tilde{\omega}'_5 + \vartheta_\nu$, $\tilde{\omega}'_6 + \vartheta_\nu$, $\Omega' + \vartheta_\nu + \vartheta_z$, writing

$$\mathscr{H}_1 = \mathscr{H}_5(\tilde{\omega}'_5 + \vartheta_\nu) + \mathscr{H}_6(\tilde{\omega}'_6 + \vartheta_\nu) \\ + \mathscr{H}_{16}(\Omega' + \vartheta_\nu + \vartheta_z) + (\mathscr{H}_1 - \mathscr{H}_5 - \mathscr{H}_6 - \mathscr{H}_{16}),$$

and we separately study the integrable models

$$\mathscr{H}_{\nu_5} = \mathscr{H}_0 + \mathscr{H}_5 \quad (17)$$

for the case of the ν_5 resonance,

$$\mathscr{H}_{\nu_6} = \mathscr{H}_0 + \mathscr{H}_6 \quad (18)$$

for the ν_6 resonance, and

$$\mathscr{H}_{\nu_{16}} = \mathscr{H}_0 + \mathscr{H}_{16} \quad (19)$$

for the ν_{16} resonance. For each of these models, we evaluate the separatrices in the (q_{crit}, Θ_σ, Θ_z, Θ_ν) space, where q_{crit} is respectively equal to $\tilde{\omega}'_5 + \vartheta_\nu$, $\tilde{\omega}'_6 + \vartheta_\nu$, and $\Omega' + \vartheta_\nu + \vartheta_z$.

In addition, we compute the location in the (Θ_σ, Θ_z, Θ_ν) action space of the resonances up to order 5 among $\dot{\vartheta}_\sigma$, $\dot{\vartheta}_z$, $\dot{\vartheta}_\nu + g_5$, $\dot{\vartheta}_\nu + g_6$, and $\dot{\vartheta}_\nu + \dot{\vartheta}_z + s_6$, which are a generalization of the *secondary resonances* (Lemaître and Henrard 1990) for the three-dimensional secular problem (4). The time derivatives of the angles ϑ_σ, ϑ_z, and ϑ_ν are computed as

$$\dot{\vartheta}_\sigma = \frac{\partial \mathscr{H}_0}{\partial \Theta_\sigma}, \qquad \dot{\vartheta}_z = \frac{\partial \mathscr{H}_0}{\partial \Theta_z}, \qquad \dot{\vartheta}_\nu = \frac{\partial \mathscr{H}_0}{\partial \Theta_\nu}. \quad (20)$$

Finally, inverting the relations (14), (9), and (3), we compute the separatrices of the ν_5, ν_6, ν_{16}, Kozai and 2/1 resonance as well as the location of the secondary resonances in the (a, e, i)-space. In doing this, we need to fix the values of the critical angles of the various resonances. As a rule, the separatrices of each secular resonance are computed for the value of the critical secular resonant argument corresponding to the largest separatrix separation. The results are represented in Fig. 1, and they will be discussed in the next section.

Although simple in principle, the procedure illustrated above is technically complicated. In the evaluations of the averaged Hamiltonian (4) and its derivatives, we cannot use the classical series expansions in powers of the asteroid
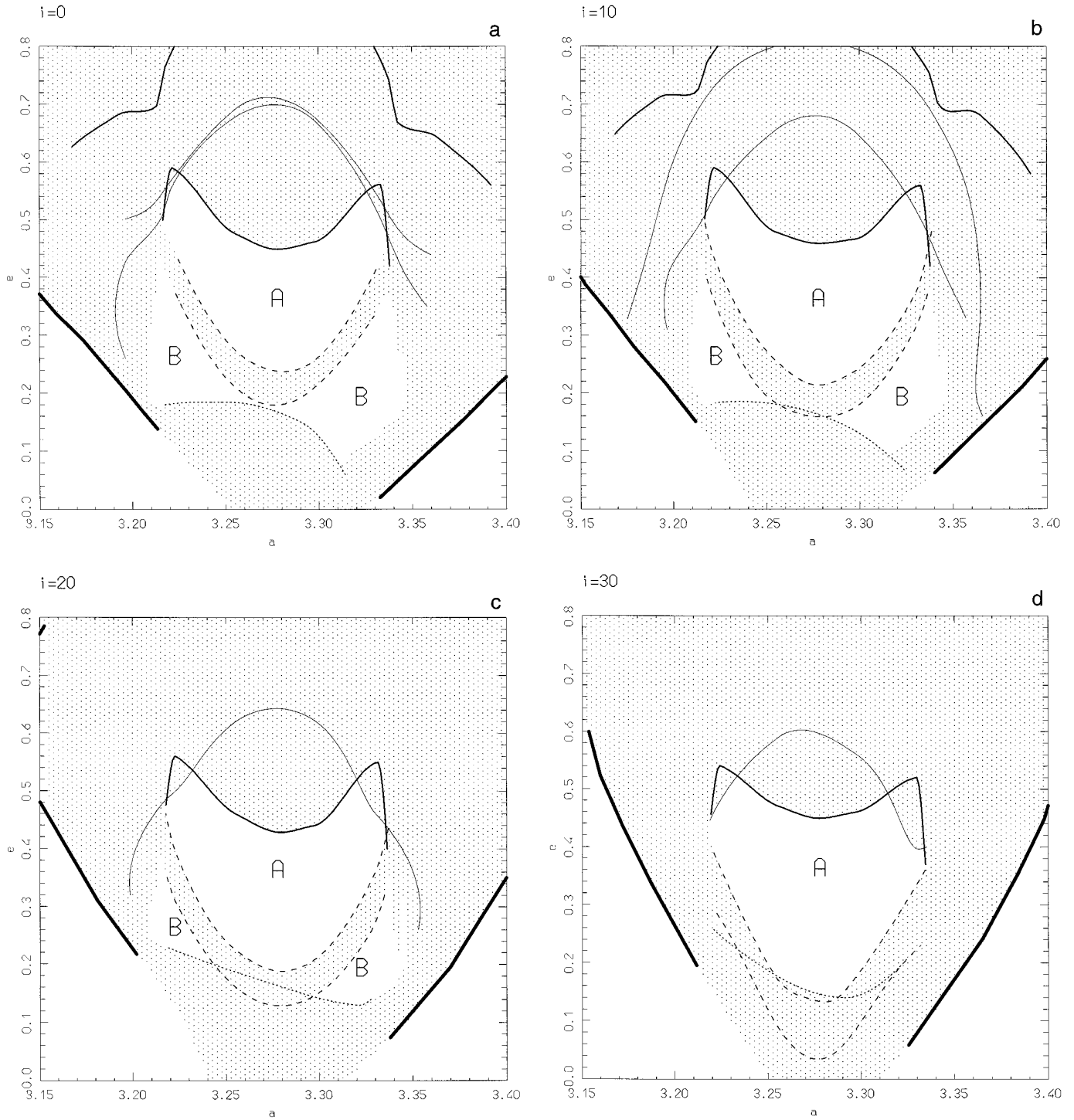
FIG. 1. Strongly chaotic regions (dotted) and quasi-regular islands (white areas denoted by A and B) in the 2/1 resonance at different inclinations. The two thick lines on the sides denote the separatrices of the 2/1 mean-motion resonance; the short dashed curve marks the upper limit of the secondary resonances; the long dashed, solid, and bold curves denote, respectively, the separatrices of the ν_{16}, Kozai, and ν_5 resonances. See text for comments.

eccentricity and inclination; otherwise results would lose accuracy for large values of e or (less critically) of i. Instead of that, we are going to use the techniques of local evaluation developed in Moons (1993, 1994). Conversely, we expand the Hamiltonian with respect to Jupiter's eccentricity e' and inclination i' up to first order. Such expansion simplifies the computations a great deal. Indeed the zero-order part is independent of $\tilde{\omega}_5'$, $\tilde{\omega}_6'$, and Ω' (and therefore, for the D'Alembert characteristics, is also independent of ν or ψ_ν). In the linear part, the terms in $\tilde{\omega}_5'$, $\tilde{\omega}_6'$, and Ω' are naturally separated and each of them has zero average. Therefore in (7) and (12) the integrals over $\tilde{\omega}_5'$, $\tilde{\omega}_6'$, and Ω' are simply equal to the zero-order part in e' and i'. Conversely, the integral over σ_z in (7) and the one over ψ_σ in (12) need to be computed numerically. A further complication is that, as discussed by Henrard (1990), the introduction of angle-action variables, as in (9) and (14), cannot be done explicitly, but requires semi-numerical techniques. We use a 3-D adaptation of the software developed in Morbidelli (1993), which numerically evaluates coordinate transformations and Hamiltonian terms over grids in the action space and interpolates the computed data on the grid nodes.

3. 3-D DYNAMICAL STRUCTURE OF THE 2/1 COMMENSURABILITY

Following the perturbation approach sketched in the previous section, we estimated the structure of the secular dynamics inside the 2/1 mean-motion resonance.

Our results are illustrated in Fig. 1. Since the (a, e, i)-space is three-dimensional, the four panels show the dynamical structure of the (a, e) plane at increasing inclination levels. We are now going to discuss the meaning of the various curves and symbols.

• The two thick lines on the sides denote the separatrices of the 2/1 mean-motion resonance, computed for the resonant critical argument $\sigma = 0$. We recall that in this paper, we are going to investigate the dynamics only *inside* the 2/1 resonance, namely in the region bounded by the two separatrices.

• The short dashed curve marks the upper limit of the region concerned by the presence of secondary resonances of order not larger than 5. Recall that, while in the planar–elliptic problem secondary resonances are defined by the rational ratio between the libration period of σ and the circulation period of $\tilde{\omega}$ (Lemaître and Henrard 1990), in the 3-D secular problem there are different families of secondary resonances and indeed here we have studied four of them. More precisely, denoting by $\dot{\vartheta}_\sigma$ the libration frequency in the 2/1 resonance, by g the proper frequency of $\tilde{\omega}$, by s the proper frequency of Ω, and by g_5, g_6, and s_6 Jupiter main proper frequencies, we have considered the families of secondary resonances defined by

$$\dot{\vartheta}_\sigma = k(g - g_5), \qquad \dot{\vartheta}_\sigma = k(g - g_6),$$
$$\dot{\vartheta}_\sigma = k(g - s), \qquad \dot{\vartheta}_\sigma = k(s - s_6),$$

with $|k| \leq 5$. As a matter of fact the last family does not exist since everywhere $|\dot{\vartheta}_\sigma| > 5|s - s_6|$.

• The long dashed curves denote the separatrices of the ν_{16} resonance; we recall that it occurs when $s = s_6$.

• The solid curves refer to the Kozai-resonance separatrix. Recall that the Kozai resonance concerns the libration of the perihelion argument ω and hence it occurs when $g = s$.

• The bold curves denote the separatrices of the ν_5 resonance ($g = g_5$).

• The ν_6 secular resonance ($g = g_6$) is also present inside the 2/1 commensurability: it is always located above the ν_5 and partially overlaps with the former). We do not report the separatrices of the ν_5 resonance for sake of simplicity.

• The points color the regions concerned by either the above discussed secular or secondary resonances. This is aimed at highlighting the regions where we expect strong (chaotic) variation of the orbital elements. With some arbitrariness, we have extrapolated the secular resonance separatrices in the regions where, for technical reasons, we have not been able to track them. Of course we do not expect that the effects of chaos are the same all over the dotted region. Between the long dashed curves, chaos should produce mainly large variations of the inclination, because the ν_{16} resonance is the principal actor. Below the short dashed curve, the secondary resonances should act mainly on the libration amplitude of the 2/1 resonance, with possible changes of eccentricity and inclination. The remaining region is characterized by large variations of the eccentricity because of the presence of secular resonances involving the perihelion frequency.

We can now proceed with the discussion about the content of Fig. 1 and illustrate the 3-D dynamical structure of the 2/1 resonance. This will also make it possible to review several results scattered among the so far published literature.

First of all, we remark that, with the increase of the inclination, the separatrices of the 2/1 commensurability moderately shrink. This was already pointed out by Morbidelli *et al.* (1993).

The width of the Kozai resonance increases with the inclination. This is not an astonishing fact since the coefficient of the Kozai harmonic is proportional to $e^2 i^2$ at low e and i. At $i \geq 20°$ the upper Kozai separatrix is outside of the eccentricity range covered by the figure, so that only the lower separatrix is plotted.

The ν_{16}-resonance location moves to smaller eccentricity with increasing i, therefore interacting more and more strongly with the secondary resonances complex. The increasing amplitude of the Kozai resonance and the migra-

tion of the ν_{16} resonance have been already pointed out by Morbidelli and Moons (1993) for orbits with small amplitude of σ-libration, a result extended by Henrard *et al.* (1995) to moderate amplitudes.

The Kozai resonance interacts deeply with the ν_5 resonance (and with the ν_6, not shown in Fig. 1). Partial overlap is visible at all inclinations and this is expected to lead, following Chirikov criterion (Chirikov 1960), to large-scale chaos. Such a chaos should cover all regions at large eccentricity and at large-libration amplitude, following the location of the above-mentioned resonances. This phenomenon, restricted only on the plane $i = 0$, was already shown by Morbidelli and Moons (1993).

The ν_{16} resonance interacts also with the Kozai–ν_5–ν_6 complex at moderate libration amplitude, as pointed out by Henrard *et al.* (1995).

The dotted region which, as stated above, is expected to be strongly chaotic since it is concerned with low-order secular or secondary resonances, extends almost all over the 2/1 resonant space; Fig. 1 provides the first three-dimensional picture of its extension. Only the islands denoted by A and B seem to be not affected by low-order resonances so that they should be much more regular than the rest of the 2/1 resonant phase space. The A island has already been established numerically by Ferraz-Mello (1994) and analytically by Henrard *et al.* (1995), while the existence of the B island close to the plane $i = 0$ has been previously pointed out numerically by Franklin (1994) and Morbidelli (1996, called "slowest diffusion island" in that paper). Nesvorný and Ferraz-Mello (1997) found both islands in their numerical exploration and introduced the "A" and "B" notations that we adopt here. Figure 3 in Nesvorný and Ferraz-Mello (1997) is actually very similar to our Fig. 1a, confirming the accuracy of our complicated perturbation computations. Morbidelli (1996) and Nesvorný and Ferraz-Mello (1997) numerically show that neither the A nor the B islands are really regular: all orbits in these islands slowly diffuse in phase space and escape on time scales of several hundred Myr. In this paper we are unable to understand theoretically the reason for such slow diffusion. This is probably due to high-order secondary or secular resonances, also involving the 5/2 quasi-mean motion resonance with Saturn (Ferraz-Mello and Michtchenko 1997, Michtchenko and Ferraz-Mello 1997), which are beyond the limits of our analysis.

The B island shrinks and then disappears at $i > 20°$. This allows fast escapes from the low-eccentricity region to the large-eccentricity region. At lower inclination, such escapes are prevented because the B island should be crossed. Note that in the low-eccentricity region the families of secondary resonances defined by $\dot{\vartheta}_\sigma = k(g - s)$ can excite the inclination, so that particles starting at low-i and low-e can increase first their inclination, reaching the level where the B island disappears, and hitherto evolve to large

eccentricities, as first shown numerically by Wisdom (1987). Henrard *et al.* (1995) described in detail, through a series of numerical experiments, such a "bridge" over the regular island. Figure 1 gives a clear global description of the important phenomenon of bridging over the B island, which explains the depletion of the low-eccentricity part of the 2/1 resonance (recall that in the planar elliptic problem low-e orbits, although chaotic, are bounded by invariant trajectories, so that they cannot escape; Froeschlé and Scholl 1976).

4. THE 2/1 KIRKWOOD "GAP"

The existence of a gap associated to the 2/1 mean-motion resonance has been considered a "mystery" for a long time.

Figure 1 shows that a large part of the resonance is strongly chaotic (dotted region); test particles initially placed in the dotted region—with exception of those located solely in the ν_{16} resonance—escape to large eccentricities in less than 100 Myr (Morbidelli 1996).

The depletion of the A and B islands is more problematic. Numerical integrations show that all orbits diffuse chaotically, and most escapes occur on time scales of 10^8–10^9 years (Morbidelli 1996). Since this time scale is a few times shorter than the age of the Solar System, this can possibly explain the depletion of primordial bodies in these quasi-regular islands. Besides, it has been suggested (Ferraz-Mello and Michtchenko 1997, Michtchenko and Ferraz-Mello 1997, Nesvorný and Ferraz-Mello 1997) that the A and B islands could have been much more chaotic in the past than at the present time. Indeed, the period of Jupiter–Saturn great inequality (i.e., the period of circulation of the angle $2\lambda_J - 5\lambda_S$) decreases with the Jupiter–Saturn distance, so that during the Jupiter and Saturn diverging orbital migration (Fernandez and Ip 1984) it should have been significantly shorter than the present value (880 years). In particular, if the great inequality period had slowly evolved through the values of 390 and 430 years, it would have been temporarily in 1/1 resonance with the libration period in the B and the A islands respectively, thus destabilizing such regions. This is an additional argument to explain why the central part of the 2/1 resonance is depleted of primordial asteroids.

Anyway, the 2/1 resonance is not completely empty of bodies. In addition to a small number of objects with evident irregular motion, which probably are only temporarily associated with the 2/1 resonance, Morbidelli (1996) found four asteroids in the B island. These are 3789 Zhongguo, 1975 SX, 1990 TH_7, and 1993 SK_3. Their quite small size ($\sim$10 km) makes their collisional lifetime shorter than the age of the Solar System, so that they should not be primordial asteroids. A numerical integration of their evolution over 850 Myr shows that the last three asteroids do not leave the B island on the integration time span (although

chaotically diffusing around), while 3789 Zhongguo escapes in 300 Myr. Note also that, because of the chaotic character of the evolutions, these integrations are not deterministic and should be interpreted just as an indication of the typical dynamical lifetimes of these objects. In this paper we have searched through the catalog of the asteroids which have been discovered after 1993; we have numerically integrated for 3 Myr all those whose orbit has been determined over an observational arc longer than 1 year and we have found an additional asteroid, 1994 UD$_1$, also in the B island. Interestingly, no asteroid has been found in the A island up to now (Nesvorný and Ferraz-Mello 1997).

What is the origin of these five asteroids and why is the A island empty of sizeable objects? A tempting conjecture is that they are the remnants of the Themis family breakup, which certainly injected many family members into the 2/1 resonance (Morbidelli *et al.* 1995). Since 1995 we have explored this hypothesis more quantitatively. The breakup of the Themis family has been simulated, extrapolating the ejection velocity field which characterizes the presently recovered family (Zappalà *et al.* 1996). Then, the evolutions of fictitious family members inside or close the 2/1 resonance have been numerically integrated for 100 Myr in the framework of the GAPTEC project (Gladman *et al.* 1997). The integrations have been done using the "swift" code (Levison and Duncan 1994) and in the framework of a realistic Solar System including the planets from Venus to Neptune. In the present paper, for each of the integrated fictitious family members, we have computed the initial diffusion speed in the following way:

(1) We evaluated the proper eccentricity at 1-Myr time intervals, averaging the osculating eccentricity (output every 500 years) over 1 Myr.

(2) We estimated the time span $[0, T]$ such that $|e_{\text{proper}}(t) - e_{\text{proper}}(0)]| < 0.02$ for all $t \leq T$. Since we are interested in the diffusion speed in the neighborhood of the initial orbit, and we do not want any contamination by the last stages of the escape process, where usually diffusion accelerates since the orbit has reached the large-eccentricity strongly chaotic region.

(3) We calculated the best-fit line for the $e_{\text{proper}}(t)$ data as a function of t on the time span $[0, T]$.

(4) We assumed the slope of such a line as a measure of the diffusion speed.

In Fig. 2 we report the initial conditions (corresponding to $\sigma = 0$ and $\tilde{\omega} - \tilde{\omega}' = 0$) of the fictitious family members, while the size of each polygon is proportional to the square root of their diffusion speed. As a magnification of Fig. 1a,[1] the separatrices of the 2/1 resonance (thick lines), the
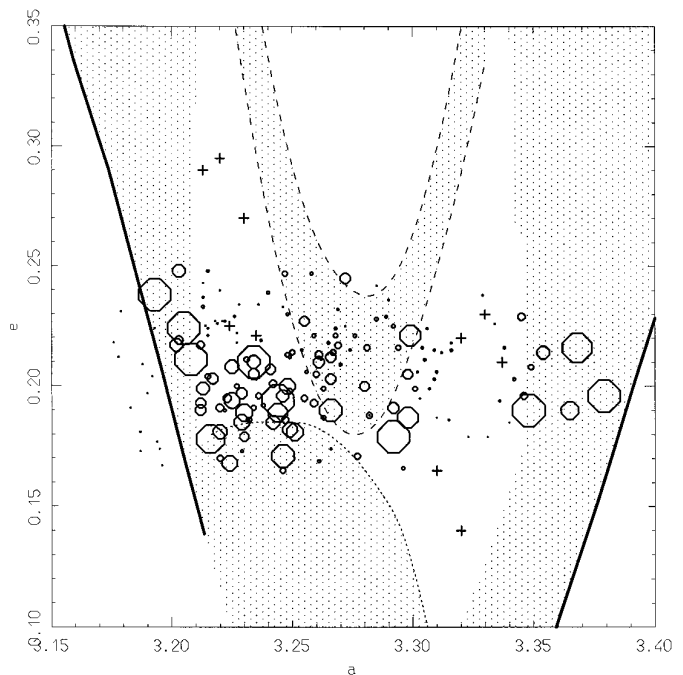

FIG. 2. Magnification of Fig. 1a. Polygons denote the initial conditions of fictitious Themis-family ejecta, the evolution of which has been numerically computed in Gladman *et al.* (1997). The size of each polygon is proportional to the numerically computed diffusion speed. Crosses denote the position (on both side of the resonance) of the five recently discovered asteroids.

separatrices of the ν_{16} resonance (long dashed curves), and the upper border of the secondary resonances region (short dashed curve) are also plotted, together with the dotted area, denoting the expected strongest chaotic region. We remark that the sizes of the polygons are roughly in good agreement with the dotted area, the smallest polygons (corresponding to the most regular orbits) being deep in the B island or outside the 2/1 resonance. The most important discrepancy is that polygons of nonnegligible size are present also *above* the short dashed curve delimiting the secondary resonances region at ~3.23 AU. This is mainly due to the fact that the plotted initial conditions of the fictitious family members correspond to $\tilde{\omega} - \tilde{\omega}' = 0$, whereas the border of the secondary resonance region (and of the ν_{16} secular resonance) are evaluated in coordinates which are averaged over $\tilde{\omega} - \tilde{\omega}'$ (see Section 2). The choice of the phase $\tilde{\omega} - \tilde{\omega}' = 0$ would move the secondary resonance border about 0.02 higher in eccentricity.

In Fig. 2 the crosses denote the (a, e) elements of the five asteroids in the B island, computed at $\sigma = \tilde{\omega} - \tilde{\omega}' = 0$ on both sides of the resonance. Comparing the positions of the real asteroids with those of the simulated particles ejected from the Themis family, we remark that, *from an orbital point of view*, the five asteroids in the B island could be Themis-family survivors: two of them injected on the

---

[1] The computation is done for $i = 0$ because of the small inclination of the Themis family and of the five asteroids in the B-island.

left side of the resonance and three on the right side. Also the inclinations of family particles and of the asteroids are very similar, confirming this hypothesis.

It should be qualified that such a good agreement is due to the choice of the value of $\tilde{\omega} - \tilde{\omega}'$ at the moment of the simulated breakup. The eccentricity of the asteroid 24 Themis oscillates approximately between 0.1 to 0.2, the first value corresponding to $\tilde{\omega} - \tilde{\omega}' = 180$, the second to $\tilde{\omega} - \tilde{\omega}' = 0$. Conversely, the eccentricities of the asteroids in the 2/1 resonance and the location of secondary resonances do not change so much with the circulation of the argument $\tilde{\omega} - \tilde{\omega}'$, because of the much larger frequency of $\tilde{\omega}$. Therefore, simulating the Themis breakup at $\tilde{\omega} - \tilde{\omega}' = 180$ would result in injecting the fictitious family members mainly in the secondary resonances region, without covering the positions of the observed asteroids.

The five asteroids in the B island have absolute magnitudes ranging from 12.8 to 13.5 so that, assuming the albedo of the Themis family members, they should have diameters between 8 and 13 km (with a typical error of about 4 km). Zappalà *et al.* (1997) estimate that the Themis family breakup event should have injected in the 2/1 resonance about 380,000 asteroids larger than 1 km, 600 larger than 5 km, and 15 larger than 10 km. Since about 1/3 of the simulated injected particles fall in the B island (those denoted by small polygons), we would expect that about five asteroids larger than 10 km should have been injected there. This number seems to be somewhat small: in fact five asteroids have been discovered up to now, but, taking into account that at 3.27 AU the completeness limit of detectability is approximately 24.7 km, we expect that several more will be discovered in the future. However, being the size distribution of the injected objects being very steep, the numbers become consistent if the observed asteroids are somewhat smaller than 10 km. Therefore, although a definite conclusion cannot be reached by now, the model in which the five asteroids in the B island are Themis family survivors could be viable also *from the size distribution point of view*.

Such a model would also explain why no asteroids have been discovered up to now in the A island. As a matter of fact, whatever could be the angle ($\tilde{\omega} - \tilde{\omega}'$) at the moment of breakup, 24 Themis could not have injected sizeable asteroids at such a large eccentricity, given the ejection velocity field characterizing the observed family.

5. THE 2/1 RESONANCE AS A SOURCE OF METEORITES

Although it is impossible to dynamically deplete the entire 2/1 resonance on a short time scale, it should not be forgotten that there are strongly chaotic portions which lead to Earth-crossing orbits in a few million years.

To stress this point, we show in Fig. 3 the dynamical lifetimes of the test particles integrated in the GAPTEC
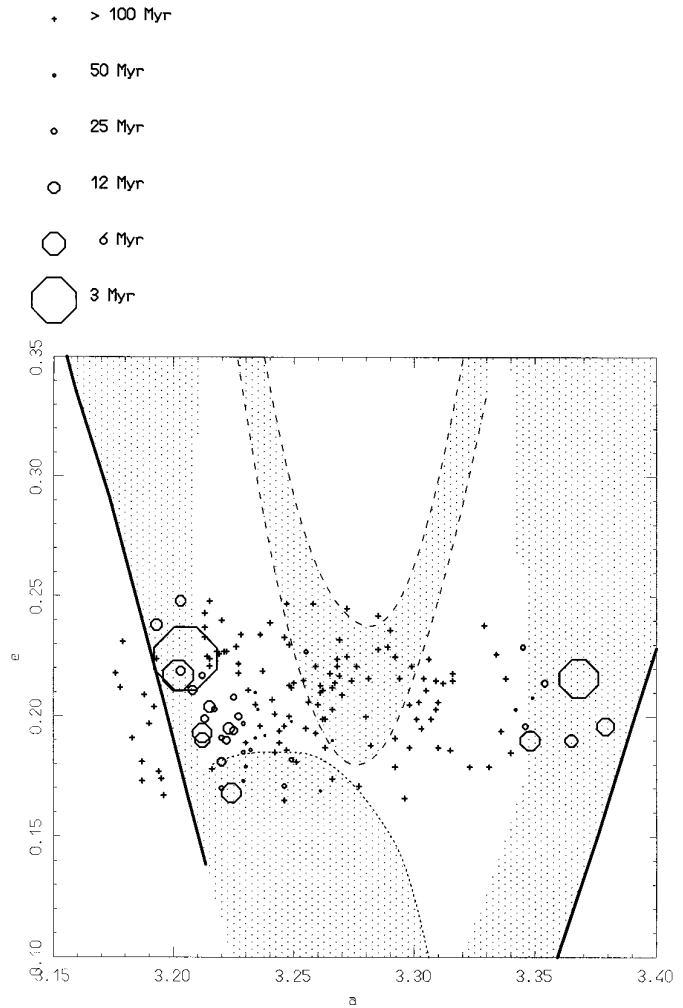

FIG. 3. The same as Fig. 2, but the size of each polygon is inversely proportional to the time required to become an Earth crosser. Crosses denote particles which never become Earth crossing within the 100-Myr integration length of Gladman *et al.* (1997).

project (Gladman *et al.* 1997). Figure 3 is the same as Fig. 2, but the size of the polygon is now inversely proportional to the time required to become Earth crosser. The crosses denote the particles which survive the 100-Myr integration.

Remark that the particles in the large amplitude libration region typically become Earth crossers in less than ∼10 Myr, which is of the order of the typical collisional lifetime of meteoroids (Morbidelli and Gladman 1997). It should be considered that the left side of the 2/1 resonance is densely populated with asteroids (mainly because of presence of the Themis and the Hygiea families) and that most of the material continuously injected into the resonance by the neighboring asteroids preferentially falls into the region where the required ejection velocities are lowest. For their spectroscopical properties, the asteroids close to the 2/1 resonance could be parent bodies of the Cl or CM

meteorites. In particular, Hiroi *et al.* (1996) have pointed out the spectroscopical similarities of 511 Davida and B-7904, 10 Hygiea and Y-82162, and 130 Elektra and LEW-90500. Therefore it is tempting to conjecture that the 2/1 resonance can be an efficient source of CI/CM meteorites.

As in Morbidelli and Gladman (1997), for each of the simulated particles which ever become Earth crossing, we have computed the total Earth-collision probability. This has been done as follows: we have taken the time history of the orbital elements a, e, and i provided by the numerical integration, and for every set $(a, e, i)(t)$ we have computed the collision probability with the Earth $P(t)$ and the average impact velocity $V(t)$, averaging over all possible orbital configurations occurring during a precessional cycle of the orbits and taking into account the Earth gravitational focusing (Manley and Migliorini 1997). The total collision probability P_{Tot} is then computed using the formula

$$P_{\mathrm{Tot}} = \sum_t P(t) 2^{-t/\tau} C(t).$$

In the formula above, the exponential $2^{-t/\tau}$ introduces the "probability to exist" that the particle has at time t due to a finite collisional half-life τ; we have assumed $\tau = 10$ Myr as in (Morbidelli and Gladman 1997). The factor $C(t)$ if equal to 1 if $V(t)$ is smaller than a given threshold value, and is 0 otherwise, taking into account that there is an entry velocity bias on the recovery of meteorites at ground; we have assumed a threshold of 20 km/s in agreement with Wetherill and ReVelle (1981) on chondritic fireballs, which is probably optimistic for carbonaceous meteorites.

The result is such that, on average, particles which become Earth crossers have a collision probability with our planet equal to 1.5×10^{-6}. This number is 400 times smaller than the one obtained for particles initially placed in the 3 : 1 and 3000 times smaller than the one related to particles initially in the ν_6 resonance (Morbidelli and Gladman 1997). This is due basically to several reasons: (i) particles from the 2 : 1 resonance take on average a longer time to become Earth crossers than those from the above-quoted resonances, so that a more relevant fraction of meteorite-sized objects are collisionally destroyed before having a chance to encounter our planet; (ii) the time spent in Earth-crossing orbit by meteoroids coming out of the 2/1 resonance is, on average, shorter than for those from the 3 : 1 or the ν_6 resonance, since some of the latter live several millions of years in orbits with semi-major axes smaller than 2 AU; (iii) the region of the (a, e, i) space allowed by the atmosphere entry velocity bias is much smaller at 3.3 AU than at 2.1 or 2.5 AU, so that Earth-crossing meteoroids close to the 2/1 resonance typically encounter our planet with a relative speed which does not allow the delivery of a ground recoverable meteorite; (iv) the probability

of collision with the Earth decreases with increasing semi-major axis.

The CI and CM meteorites represent, respectively, 0.6 and 2.2% of the total number of recovered meteorites (Sears and Dodd 1988), but the fraction impacting the high atmosphere should be much larger, since carbonaceous meteorites are very fragile and reach the ground with much difficulty. Therefore, since most of the meteorites (i.e., the chondrites) are expected to come from the 3:1 and ν_6 resonances, the source resonance of the CI/CM meteorites should have an efficiency not much smaller than that of 3:1 and ν_6. The fact that the Earth-collision probability of the particles from the 2/1 resonance is less than 1% of that of the particles from 3:1 and ν_6 indicates that the 2/1 resonance should not be regarded as the dominating source of such meteorites.

Possible alternative parent bodies of CM meteorites have been recently pointed out in the vicinity of the 3:1 resonance (Burbine 1998).

6. CONCLUSIONS

In the present paper we provide a picture of the three-dimensional dynamical structure of the 2/1 resonance using semi-analytic techniques. Our results are in agreement with those of the several previous numerical explorations.

We show that, from the oribital viewpoint, the five asteroids which are in a quasi-stable island of the 2/1 resonance could be members of the Themis asteroid family. These asteroids could have been injected into the resonance by the family formation event. This conjecture can also be supported from the point of view of size distribution, in particular if it is confirmed that the discovered asteroids are somewhat smaller than 10 km.

We also explore the possibility that the 2/1 resonance is a major transport route for CI and CM meteorites, but we find that the collision probability with the Earth of the particles which become Earth-crossing is too low to account for the observed relative abundance of such meteorites. Some CI or CM meteorites could come from asteroids close to the 2/1 resonance but the vicinity of the resonance should not be the dominating source.

REFERENCES

Arnold, V. I. 1963. On a theorem of Liouville concerning integrable problems of dynamics. *Sib. Mathem. Zh.* **4,** 2–10.

Burbine, T. H. 1998. Could G-class asteroids be the parent bodies of CM meteorites? *Meteoritics Planet. Sci.* **33,** 253–259.

Chirikov, B. V. 1960. Resonance processes in magnetic traps. *Plasma Phys.* **1,** 253–260.

Fernandez, J. A., and W. H. Ip 1984. Some dynamical aspects of the accretion of Uranus and Neptune: The exchange of the orbital angular momentum with planetesimals. *Icarus* **58,** 109–120.

Ferraz-Mello, S. 1994. Dynamics in the asteroid 2/1 resonance. *Astron. J.* **108,** 2330–2337.

Ferraz-Mello, S., and T. A. Michtchenko 1997. Orbital evolution of the asteroids in the Hecuba gap. In *The Dynamical Behaviour of Our Planetary System* [in press]. Kluwer, Dordrecht.

Franklin, F. A. 1994. An examination of the relationship between chaotic orbits and the Kirkwood gap at the 2 : 1 resonance. *Astron. J.* **107,** 1890–1899.

Froeschlé, C., and H. Scholl 1976. On the dynamical topology of the Kirkwood gaps. *Astron. Astrophys.* **48,** 389–393.

Giffen, R. 1973. A study of commensurable motion in the asteroid belt. *Astron. Astrophys.* **23,** 387–403.

Gladman, B. J., F. Migliorini, A. Morbidelli, V. Zappalà, P. Michel, A. Cellino, Ch. Froeschlé, H. Levison, M. E. Bailey, and M. Duncan 1997. Dynamical lifetimes of objects injected into asteroid main belt resonances. *Science* **277,** 197–201.

Henrard, J. 1990. A semi-numerical perturbation approach for separable Hamiltonian systems. *Celest. Mech.* **49,** 43–68.

Henrard, J., and A. Lemaître 1983. A mechanism of formation for the Kirkwood gaps. *Icarus* **55,** 482–494.

Henrard, J., N. Watanabe, and M. Moons 1995. A bridge between secondary and secular resonances inside the Hecuba gap. *Icarus* **115,** 336–346.

Hiroi, T., M. E. Zolensky, C. M. Pieters, and M. E. Lipschutz 1996. Thermal metamorphism of the C, G, B, and F asteroids seen from the 0.7 micron, 3 micron, and UV absorption strengths in comparison with carbonaceous chondrites. *Meteoritics Planet. Sci.* **31,** 321–327.

Jefferys, W. H., and E. M. Standish 1972. Further periodic solutions of the three dimensional restricted problem. *Astron. J.* **77,** 394–400.

Laskar, J. 1996. Introduction to frequency map analysis. In *Proceedings of the NATO Advanced Study Institute 3DHAM95* [in press]. Kluwer, Dordrecht.

Lemaître, A., and J. Henrard 1990. On the origin of the chaotic motion in the 2/1 jovian resonance. *Icarus* **83,** 391–409.

Levison, H., and M. Duncan 1994. The long-term behavior of short-period comets. *Icarus* **108,** 18–36.

Manley, S. P., and F. Migliorini 1997. An algorithm for determining collision probabilities between small Solar System bodies. In *The Dynamical Behaviour of our Planetary System*, [in press]. Kluwer, Dordrecht.

Michtchenko, T. A., and S. Ferraz-Mello 1997. Chaotic diffusion in the 2/1 resonance. *Planet. Space Sci.* **45,** 1587–1598.

Moons, M. 1993. *Averaging Approaches*. Department of Mathematics Report, Vol. 19. FUNDP, Namur.

Moons, M. 1994. Extended Schubart averaging. *Celest. Mech.* **60,** 173–186.

Moons, M. 1997. Review of the dynamics in the Kirkwood gaps. *Celest. Mech.* **65,** 175–204.

Morbidelli, A. 1993. On the successive elimination of perturbation harmonics. *Celest. Mech.* **55,** 101–130.

Morbidelli, A. 1996. On the Kirkwood gap at the 2/1 commensurability with Jupiter: Numerical results, *Astron. J.* **111,** 2453–2461.

Morbidelli, A., and A. Giorgilli 1993. Quantitative perturbation theory by successive elimination of harmonics. *Celest. Mech.* **55,** 131–159.

Morbidelli, A., and B. J. Gladman 1997. Orbital and temporal distribution of meteorites originating in the asteroid belt. *Meteoritics Planet. Sci.*, in press.

Morbidelli, A., and M. Guzzo 1996. The Nekhoroshev theorem and the asteroid belt dynamical system. *Celest. Mech.* **65,** 107–136.

Morbidelli, A., and M. Moons 1993. Secular resonances inside mean motion commensurabilities: The 2/1 and 3/2 cases. *Icarus* **103,** 99–108.

Morbidelli, A., Ch. Froeschlé, and H. Scholl 1993. The ν_6 secular resonance near the 2/1 mean motion commensurability at 3.0–3.2 A.U. *Astron. Astrophys.* **278,** 644–653.

Morbidelli, A., V. Zappalà, M. Moons, A. Cellino, and R. Gonczi 1995. Asteroid families close to mean motion resonances: Dynamical effects and physical implications. *Icarus* **118,** 132–154.

Nesvorný, D., and S. Ferraz-Mello 1997. On the asteroidal population of the first-order Jovian resonances. *Icarus* **130,** 247–258.

Nobili, A., A. Milani, and M. Carpino 1989. Fundamental frequencies and small divisors in the orbits of the outer planets. *Astron. Astrophys.* **210,** 313–336.

Sears, D. W. G., and R. T. Dodd 1988. Overview and classification of meteorites. In *Meteoritics and the Early Solar System* (J. F. Kerrige and M. Shapley Matthews, Eds.), pp. 3–31. Univ. of Arizona Press, Tucson.

Šidlichovský, M., and D. Nesvorný 1997. Frequency modified Fourier transform and its applications to asteroids. *Celest. Mech.* **65,** 137–148.

Wetherill, G. W., and D. O. ReVelle 1981. Which fireballs are meteorites? A study of the Prairie network photographic meteor data. *Icarus* **48,** 308–328.

Wisdom, J. 1987. Chaotic dynamics in the solar system. *Icarus* **72,** 241–275.

Zappalà, V., A. Cellino, A. Dell'Oro, F. Migliorini, and P. Paolicchi 1996. Reconstructing the original velocity field of asteroid families. *Icarus* **124,** 156–180.

Zappalà, V., A. Cellino, B. J. Gladman, S. Manley, and F. Migliorini 1998. Asteroid showers on Earth after family break-up events. *Icarus* **134,** 176–179.